

Theory of exciton transport in molecular crystals strongly coupled to a cavity: A temperature-dependent variational approach

Jingyu Liu,¹ Qing Zhao,¹ and Ning Wu^{1,*}

¹*Center for Quantum Technology Research, School of Physics,
Beijing Institute of Technology, Beijing 100081, China*

We present a semianalytical theory for exciton transport in organic molecular crystals interacting strongly with a single cavity mode. Based on the Holstein-Tavis-Cummings model and the Kubo formula, we derive an exciton mobility expression in the framework of a temperature-dependent variational canonical transformation, which can cover a wide range of exciton-vibration coupling, exciton-cavity coupling, and temperatures. A closed-form expression for the coherent part of the total mobility is obtained in the zeroth order of the exciton-vibration coupling. By performing numerical simulations on both the H- and J-aggregates, we find that the exciton-cavity has significant effects on the total mobility: 1) At low temperatures, there exists an optimal exciton-cavity coupling strength for the H-aggregate at which a maximal mobility is reached, while the mobility in the J-aggregate decreases monotonically with increasing exciton-cavity coupling; 2) At high temperatures, the mobility in both types of aggregates get enhanced by the cavity. We illustrate the above-mentioned low-temperature optimal mobility observed in the H-aggregate by using realistic parameters at room temperature.

I. INTRODUCTION

Exciton diffusion in molecular materials is a fundamental process relevant to a variety of physical phenomena, including organic semiconductors [1], solar cell physics [2], and excitation energy transfer in natural/artificial light-harvesting systems [3, 4], etc. In particular, the exciton transport in molecular crystals has been a long-studying topic dating back to the early theoretical investigations by Silbey and co-workers in the 1970's [5–10]. In contrast to conventional inorganic crystals which can be described by band transport, phononic/vibrational degrees of freedom have to be included in the description of charge transport in organic crystals. The transport properties in organic molecular crystals generally depend on a variety of factors, including the electronic transfer integrals between the excitons (or the electronic bandwidth), the electron-phonon coupling strength, the characteristic frequency of the phonons, and temperature, etc.

Typical theoretical investigations on the charge-carrier transport in molecular crystals are usually based on the famous Holstein Hamiltonian [11], and various theoretical methods were developed to treat the dynamics of the Holstein model (see Refs. [1, 12] and references therein). Among these, the (variational) polaron transformation and its generalizations offers a promising approach to deal with the problem at a broad range of parameters [7, 8, 10, 14–17]. In particular, Cheng and Silbey developed a finite-temperature variational approach by combining Merrifield's transformation with Bogoliubov's bound on the free energy of the composite system [15]. Based on the polaron transformation, Ortmann *et al.*

presented a theoretical description of charge transport in molecular crystals and derived a mobility expression using the Kubo formula [16].

Recently, the demonstration of strong coupling between confined light fields and organic matter has stimulated intensive interest in experimental/theoretical investigations of strong-coupling effects on charge-carrier transport [18–28]. Although in the framework the pure exciton model a dramatic enhancement of the exciton-type transport in organic materials has been revealed [18–20], it is recognized that intramolecular vibrational mode should be included to obtain a more realistic description of the system [26–33]. The such obtained composite system involving excitonic, phononic, and photonic degrees of freedom is described by the so-called Holstein-Tavis-Cummings model. In the framework of the Holstein-Tavis-Cummings Hamiltonian, Wu *et al.* [31] generalized the Cheng-Silbey [15] method to include the vibrational dressing of the cavity mode in the variational canonical transformation and provided a successful description of the static properties of the system. In special, a ground state involving all the excitonic, photonic, and vibrational degrees of freedom was demonstrated and named as a lower polaron polariton [31].

In this work, we present a microscopic theory of exciton transport in molecular crystals strongly coupled to a cavity by extending the formalism developed in Ref. [31] to a time-dependent scenario. Based on the Holstein-Tavis-Cummings Hamiltonian and the Kubo formula, we derive an exciton mobility expression in the framework of the temperature-dependent variational canonical transformation [31] that can cover a wide range of exciton-vibration and exciton-cavity couplings, as well as temperatures. Due to the appearance the cavity mode, the mobility has three contributions, i.e., the conventional pure exciton part, the pure cavity part, and the cross term between the two. At low temperatures, it is found that the mobility in an H-aggregate depends nonmonotoni-

*Electronic address: wun1985@gmail.com

cally on the exciton-cavity coupling strength. That is, there exists an optimal exciton-cavity coupling strength at which the total mobility reaches a maximum. However, for the J-aggregate we observe a monotonic decrease of the total mobility with increasing exciton-cavity coupling in the low temperature regime. These observations are explained by obtaining an analytical expression for the coherent mobility (without vibration scattering), from which we identify that the lower (upper) polaron polariton state serves as a main transport channel for exciton transport in the H-aggregate (J-aggregate). In the opposite limit with high temperatures, the mobility in both the two types of aggregates gets enhanced by the exciton-cavity coupling.

The rest of the paper is structured as follows. In Sec. II, we introduce the theoretical model and describe the generalized Merrifield variational transformation in detail. In Sec. III, we derive the expressions for the total mobility and its coherent part. In Sec. IV we present numerical examples to illustrate the application of our formalism to the exciton mobility in the H- and J-aggregates. Conclusions are drawn in Sec. V.

II. MODEL AND METHODOLOGY

A. Hamiltonian

We consider a one-dimensional molecular aggregate consisting of N monomers located in a single-mode cavity, which is described by the Holstein-Tavis-Cummings Hamiltonian ($\hbar = 1$) [26, 29–32]

$$\begin{aligned} H &= H_{\text{mat}} + H_c + H_{e-c}, \\ H_{\text{mat}} &= H_e + H_v + H_{e-v}, \\ H_e &= \sum_{n=1}^N \varepsilon a_n^\dagger a_n + J \sum_{n=1}^N (a_n^\dagger a_{n+1} + a_{n+1}^\dagger a_n), \\ H_v &= \omega_0 \sum_n b_n^\dagger b_n, H_{e-v} = \lambda \omega_0 \sum_n a_n^\dagger a_n (b_n + b_n^\dagger), \\ H_c &= \omega_c c^\dagger c, H_{e-c} = g \sum_n (a_n^\dagger c + c^\dagger a_n). \end{aligned} \quad (1)$$

The material part H_{mat} is the one-dimensional Holstein model describing the molecular aggregate with intramolecular vibrations, where J is the uniform nearest-neighbor electronic coupling. The creation operator a_n^\dagger (b_n^\dagger) creates an exciton (vibration) on site n with energy ε (ω_0). The linear exciton-vibration coupling is measured by the Huang-Rhys factor λ^2 . Note that H_{mat} can be used to describe various organic systems including molecular crystals and organic semiconductors [1, 10, 15], J- and H-aggregates [34], and light-harvesting complex II [35, 36], etc. The single-mode cavity is described by H_c , where c^\dagger creates a photon with frequency ω_c . H_{e-c} represents the uniform [37] exciton-cavity interaction with interaction strength g , where we employed the rotating wave approximation so that the total number of

excitations $\sum_n a_n^\dagger a_n + c^\dagger c$ is conserved. This is a good approximation provided the ultrastrong-coupling regime is not reached [26, 30, 31].

For simplicity, we assume periodic boundary conditions and even N throughout this work. We will work in the single-excitation subspace with $\sum_n a_n^\dagger a_n + c^\dagger c = 1$, which allows us to truncate the number of cavity photons to be at most one. The creation operators under the above single-excitation approximation can be written as $a_n^\dagger = |n\rangle\langle\text{vac}|$ and $c^\dagger = |c\rangle\langle\text{vac}|$ with $|\text{vac}\rangle$ the common vacuum of all the annihilation operators. By performing the following Fourier transform on the exciton operator, $a_n = \frac{1}{\sqrt{N}} \sum_k e^{iknd} a_k$, where $k = -\pi, -\pi + 2\pi/N, \dots, \pi - 2\pi/N$ and $d = R_{j+1} - R_j$ is the lattice spacing with R_j the position of the j th monomer, the pure exciton-photon Hamiltonian can be written in the momentum space as

$$\begin{aligned} H_e + H_c + H_{e-c} \\ = \sum_k (\varepsilon + 2J \cos k) + \omega_c c^\dagger c + g\sqrt{N}(a_0^\dagger c + c^\dagger a_0). \end{aligned}$$

We see that only the bright exciton state with zero momentum, $|k=0\rangle = a_0^\dagger|\text{vac}\rangle$, couples to the cavity field.

B. The generalized Merrifield transformation

To treat the exciton-vibration and exciton-cavity coupling at finite temperatures on an equal footing, we will employ a Merrifield transformation [15, 31] in which the variational parameters are determined by minimizing the Bogoliubov upper bound for the free energy. It has proven that the Merrifield transformation could offer an accurate description of both static [31] and dynamical properties [33] for a wide range of exciton-vibration and exciton-cavity coupling, and temperatures.

Following Ref. [31], we perform the following variational canonical transformation to H ,

$$\begin{aligned} \tilde{H} &= e^{\mathcal{S}} H e^{-\mathcal{S}}, \\ \mathcal{S} &= - \sum_n a_n^\dagger a_n B_n - c^\dagger c B_c, \end{aligned} \quad (2)$$

where

$$B_n = \sum_l f_l (b_{n+l} - b_{n+l}^\dagger), B_c = h \sum_l (b_l - b_l^\dagger). \quad (3)$$

are parameter-dependent vibrational operators. The variational parameters $\{f_l\}$ and h can be chosen real [31] and will be determined in a self-consistent way by minimizing the free energy of the transformed Hamiltonian following Bogoliubov's inequality [38],

$$F \leq F_0 + \langle \mathcal{H}_1 \rangle_{\mathcal{H}_0}, \quad (4)$$

where $\mathcal{H} = \mathcal{H}_0 + \mathcal{H}_1$ is a generic Hamiltonian and F and F_0 are the respective free energies of \mathcal{H} and \mathcal{H}_0 , and

$\langle \mathcal{H}_1 \rangle_{\mathcal{H}_0}$ represents the thermal average of \mathcal{H}_1 over the canonical ensemble defined by \mathcal{H}_0 .

Physically, the coefficient f_l (h) measures the degree of dressing of the exciton at site n (the cavity photon) by the vibrational mode on site $n + l$ (on each site). It is necessary to take the vibrational dressing of the photon into account even if the cavity is not directly coupled to the vibrations [31]. The usual full polaron transformation in the context of the Holstein model corresponds to the case of $f_l = \delta_{l0}\lambda$ and $h = 0$. By further noting that the exciton-vibration system also holds mirror symmetry, $f_l = f_{N-l}$, the number of independent variational parameters is reduced to $\frac{N}{2} + 1$, i.e., $\{f_0, f_1 = f_{N-1}, \dots, f_{\frac{N}{2}-1} = f_{\frac{N}{2}+1}, f_{\frac{N}{2}}\}$ for even N [15].

The transformed Hamiltonian \tilde{H} can be separated in a conventional way as

$$\tilde{H} = \tilde{H}_S + \tilde{V} + H_V. \quad (5)$$

Here, the system part reads

$$\tilde{H}_S = \sum_{k \neq 0} E_k a_k^\dagger a_k + [E_0 a_0^\dagger a_0 + \tilde{g}\sqrt{N}(a_0^\dagger c + c^\dagger a_0) + \tilde{\omega}_c c^\dagger c], \quad (6)$$

where

$$E_k = \varepsilon_0 + \omega_0 \left(\sum_m f_m^2 - 2\lambda f_0 \right) + 2\tilde{J} \cos k \quad (7)$$

is the renormalized exciton dispersion. The renormalized parameters appearing in \tilde{H}_S are given by

$$\tilde{J} = J\Theta_1, \quad \tilde{g} = g\Theta, \quad \tilde{\omega}_c = \omega_c + Nh^2\omega_0, \quad (8)$$

with

$$\begin{aligned} \Theta &= \langle e^{B_c - B_n} \rangle_V = e^{-\frac{1}{2} \coth \frac{\beta\omega_0}{2} \sum_l (f_l - h)^2}, \\ \Theta_{|n-n'|} &= \langle e^{B_n - B_{n'}} \rangle_V = e^{-\frac{1}{2} \coth \frac{\beta\omega_0}{2} \sum_l (f_{l-n} - f_{l-n'})^2}, \end{aligned} \quad (9)$$

where $\langle \dots \rangle_V = \text{Tr}_V \{ e^{-\beta H_V} \dots \} / \text{Tr}_V \{ e^{-\beta H_V} \}$ (with $\beta = 1/k_B T$ the inverse temperature) is the thermal average with respect to the vibrational modes. It can be seen from Eqs. (8) and (9) that the presence of the exciton-vibration decreases both the effective hopping integral J and the exciton-cavity coupling g , but increases the effective cavity frequency ω_c .

The $N - 1$ dark states $|k\rangle = a_k^\dagger |\text{vac}\rangle$ ($k \neq 0$) are decoupled from the photon and are themselves eigenstates of \tilde{H}_S , but the interaction between the bright exciton $|k = 0\rangle = a_0^\dagger |\text{vac}\rangle$ and the cavity mode leads to two branches of eigenmodes that diagonalize \tilde{H}_S ,

$$\tilde{H}_S = \sum_{k \neq 0} E_k a_k^\dagger a_k + E_U a_U^\dagger a_U + E_D a_D^\dagger a_D, \quad (10)$$

where $a_U^\dagger = C a_0^\dagger - S c^\dagger$, $a_D^\dagger = S a_0^\dagger + C c^\dagger$, and

$$E_{U/D} = \frac{E_0 + \tilde{\omega}_c}{2} \pm \sqrt{N\tilde{g}^2 + \left(\frac{E_0 - \tilde{\omega}_c}{2} \right)^2}, \quad (11)$$

with the mixing coefficients $C = \cos \frac{\theta}{2}$ and $S = \sin \frac{\theta}{2}$ determined by $\tan \theta = 2\tilde{g}\sqrt{N}/(\tilde{\omega}_c - E_0)$.

The explicit form of the residue interaction \tilde{V} can be found in Ref. [31]. By construction, the thermal average of \tilde{V} vanishes, $\langle \tilde{V} \rangle_V = 0$. By setting \mathcal{H}_0 (\mathcal{H}_1) to be $\tilde{H}_S + H_V$ (\tilde{V}) in (4), we are now ready to minimize the Bogoliubov upper bound for the free energy of \tilde{H} :

$$F_B = -\frac{1}{\beta} \ln \text{Tr} e^{-\beta(\tilde{H}_S + H_V)} = -\frac{1}{\beta} \ln Z_S - \frac{1}{\beta} \ln Z_V, \quad (12)$$

where $Z_S = \sum_{\eta=\{k(\neq 0), U, D\}} e^{-\beta E_\eta}$ is the partition function for \tilde{H}_S , and Z_V is the partition function of the free vibrational modes. Since Z_V does not depend on the variational parameters, we only need to minimize $-\frac{1}{\beta} \ln Z_S$ in Eq. (12), which results in the saddle-point conditions $\{\partial Z_S / \partial f_n = 0\}$ and $\partial Z_S / \partial h = 0$ that need to be solved self-consistently (see Ref. [31] for the explicit forms of the saddle-point equations). Note that the such obtained F_B gives an upper bound for the true free energy.

III. EXCITON MOBILITY

A. Basic formulas

The mobility along the molecular chain is given by the Kubo formula [39]

$$\mu = \frac{\beta}{2eN_e} \int_{-\infty}^{\infty} dt \langle \mathcal{J}(t) \mathcal{J}(0) \rangle_H, \quad (13)$$

where $\mathcal{J}(t) = e^{iHt} \mathcal{J} e^{-iHt}$, $e(N_e)$ is the elementary charge (number) of carriers, and the average is defined as the thermal average with respect to the full Hamiltonian H as $\langle \dots \rangle_H = \text{Tr}(\dots e^{-\beta H}) / \text{Tr}(e^{-\beta H})$. The current operator is defined through the polarization operator $P = e \sum_{j=1}^N R_j a_j^\dagger a_j$ as

$$\mathcal{J} = \frac{dP}{dt} = -i[P, H] = \mathcal{J}_a + \mathcal{J}_c, \quad (14)$$

with

$$\begin{aligned} \mathcal{J}_a &= iedJ \sum_{j=1}^N (a_j^\dagger a_{j+1} - a_{j+1}^\dagger a_j), \\ \mathcal{J}_c &= -ieg \sum_{j=1}^N R_j (a_j^\dagger c - c^\dagger a_j). \end{aligned} \quad (15)$$

The two terms in Eq. (14) represent different contributions to the current operator: \mathcal{J}_a corresponds to the usual exciton hopping between nearest-neighboring sites, while \mathcal{J}_c accounts for the exchange between the excitonic and the photonic excitations. Using Eq. (2), the current-current correlation function can be reexpressed in the

Merrifield frame as

$$\begin{aligned} \langle \mathcal{J}(t)\mathcal{J}(0) \rangle_H &= \langle \tilde{\mathcal{J}}(t)\tilde{\mathcal{J}}(0) \rangle_{\tilde{H}} \\ &= \langle \tilde{\mathcal{J}}_a(t)\tilde{\mathcal{J}}_a(0) \rangle_{\tilde{H}} + \langle \tilde{\mathcal{J}}_a(t)\tilde{\mathcal{J}}_c(0) \rangle_{\tilde{H}} \\ &\quad + \langle \tilde{\mathcal{J}}_c(t)\tilde{\mathcal{J}}_a(0) \rangle_{\tilde{H}} + \langle \tilde{\mathcal{J}}_c(t)\tilde{\mathcal{J}}_c(0) \rangle_{\tilde{H}}. \end{aligned} \quad (16)$$

Here, the transformed current operators in the Merrifield frame and in the Heisenberg picture read

$$\begin{aligned} \tilde{\mathcal{J}}_a(t) &= e^{i\tilde{H}t}\tilde{\mathcal{J}}_ae^{-i\tilde{H}t} \\ &= iedJ \sum_{j=1}^N [a_j^\dagger(t)a_{j+1}(t)e^{B_{j+1}(t)-B_j(t)} \\ &\quad - e^{B_j(t)-B_{j+1}(t)}a_{j+1}^\dagger(t)a_j(t)], \end{aligned} \quad (17)$$

and

$$\begin{aligned} \tilde{\mathcal{J}}_c(t) &= e^{i\tilde{H}t}\tilde{\mathcal{J}}_ce^{-i\tilde{H}t} \\ &= -ieg \sum_{j=1}^N R_j [a_j^\dagger(t)c(t)e^{B_c(t)-B_j(t)} \\ &\quad - e^{B_j(t)-B_c(t)}c^\dagger(t)a_j(t)]. \end{aligned} \quad (18)$$

The calculation of the Heisenberg picture operators appearing in the above equations seems challenging due to the complicated form of \tilde{H} . To proceed we have to resort to approximations. To this end, we note that the zeroth order energy E_D of \tilde{H}_S provides a good approximation for the true ground state energy of \tilde{H} [31] at zero temperature. We thus adopt the zero-order Hamiltonian

$$\tilde{H} \approx \tilde{H}_0 = \tilde{H}_S + H_v, \quad (19)$$

in the calculation of the current operators. This zeroth-order approximation is also employed in Ref. [16] to

study charge transport in organic crystals in the framework the full polaron transformation. Under the approximation given by Eq. (19), the Heisenberg picture operators appearing in Eqs. (17) and (18) can be calculated as $B_j(t) = \sum_l f_l(b_{j+l}e^{-i\omega_0 t} - b_{j+l}^\dagger e^{i\omega_0 t})$ and $B_c(t) = \hbar \sum_l (b_l e^{-i\omega_0 t} - b_l^\dagger e^{i\omega_0 t})$, and $a_j(t) = \frac{1}{\sqrt{N}} \sum_{\eta=1}^{N+1} e^{iK_\eta j - i\mathcal{E}_\eta t} x_\eta f_\eta$ and $c(t) = \sum_{\eta=1}^{N+1} e^{-i\mathcal{E}_\eta t} y_\eta f_\eta$, where we introduced (for $\eta = 1, 2, \dots, N+1$) $x_\eta = \{1, \dots, 1, C, S\}$, $y_\eta = \{0, \dots, 0, -S, C\}$, $K_\eta = \{k(\neq 0), 0, 0\}$, $\mathcal{E}_\eta = \{E_{k(\neq 0)}, E_U, E_D\}$, and $f_\eta = \{a_{k(\neq 0)}, a_U, a_D\}$. In Appendix A, we list the explicit expressions for the four terms in the current-current correlation function given by Eq. (16).

B. Coherent contribution

Following Ref. [16], we separate the contributions to the mobility into a coherent part (without vibration scattering) and an incoherent part (scattering processes by the vibrations),

$$\mu = \mu^{(\text{coh})} + \mu^{(\text{inc})}, \quad (20)$$

which is achieved by splitting the thermal averages of the vibrational operators appearing in the current-current function according to, e.g., $\langle e^{B_l(t)-B_r(t)} e^{B_n-B_m} \rangle_{H_v} = 1 + [\langle e^{B_l(t)-B_r(t)} e^{B_n-B_m} \rangle_{H_v} - 1]$, where the unit corresponds to coherent transport in the zeroth order of exciton-vibration coupling and the second term corresponds to incoherent transport [16]. In Appendix B we show that only the first and the last term in the coherent contribution to the current-current correlation function, $\langle \tilde{\mathcal{J}}_a(t)\tilde{\mathcal{J}}_a(0) \rangle_{\tilde{H}}^{\text{coh}}$ and $\langle \tilde{\mathcal{J}}_c(t)\tilde{\mathcal{J}}_c(0) \rangle_{\tilde{H}}^{\text{coh}}$, survive and lead to

$$\begin{aligned} \mu^{(\text{coh})} &= \frac{\beta}{2eN_e} \int_{-\infty}^{\infty} dt e^{-(t/\tau)^2} [\langle \tilde{\mathcal{J}}_a(t)\tilde{\mathcal{J}}_a \rangle_{\tilde{H}_0}^{\text{coh}} + \langle \tilde{\mathcal{J}}_c(t)\tilde{\mathcal{J}}_c \rangle_{\tilde{H}_0}^{\text{coh}}] \\ &= \frac{\sqrt{\pi}\tau\beta e(dJ)^2}{N_e Z_S \hbar^2} \sum_{\eta=1}^{N-1} e^{-\beta E_\eta} (1 - \cos 2K_\eta) + \frac{\sqrt{\pi}\tau\beta e(dg)^2 N(N+1)^2}{8N_c Z_S \hbar^2} (e^{-\beta E_U} + e^{-\beta E_D}) e^{-\frac{1}{4}\tau^2(E_U-E_D)^2} \\ &\quad + \frac{\sqrt{\pi}\tau\beta e(dg)^2 N}{4N_e Z_S \hbar^2} \sum_{\eta=1}^{N-1} [S^2 (e^{-\beta \mathcal{E}_\eta} + e^{-\beta E_U}) e^{-\frac{1}{4}\tau^2(\mathcal{E}_\eta-E_U)^2} + C^2 (e^{-\beta \mathcal{E}_\eta} + e^{-\beta E_D}) e^{-\frac{1}{4}\tau^2(\mathcal{E}_\eta-E_D)^2}] \frac{1}{1 - \cos K_\eta d}, \end{aligned} \quad (21)$$

where we restored \hbar and introduced a finite coherence time τ due to the static disorder [16]. Note that the last two terms proportional to g^2 are due to the effect of finite exciton-cavity coupling. The coherent mobility $\mu^{(\text{coh})}$ mainly determines the low-temperature behavior of the total mobility.

IV. NUMERICAL RESULTS

A. Coherent mobility

In order to demonstrate the effect of exciton-cavity interaction, we first consider the coherent mobility for

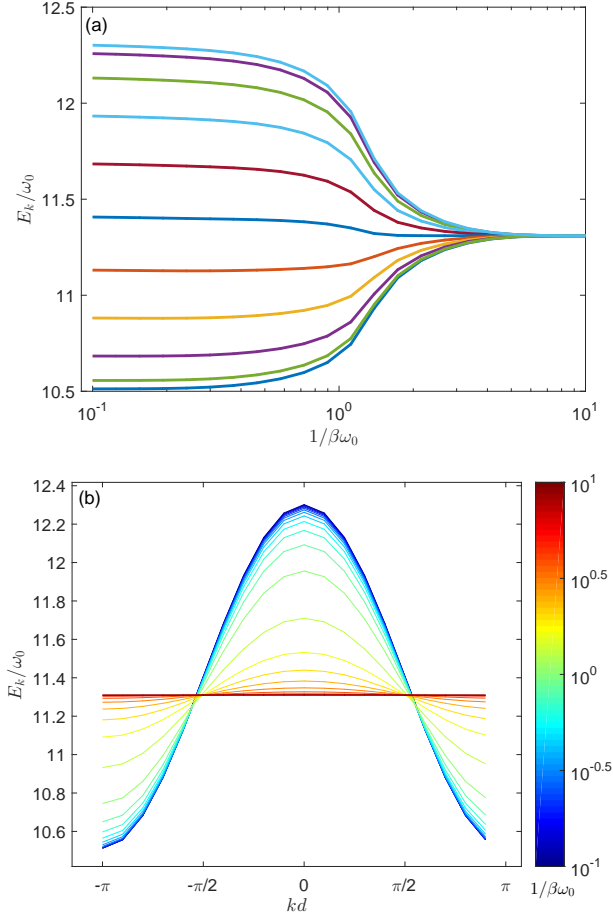


FIG. 1: (a) Renormalized exciton spectrum as a function of temperature for $N = 20$ and $g = 0$. The bandwidth narrows down as temperature increases. (b) Exciton dispersion for different temperatures. Other parameters: $\varepsilon_0/\omega_0 = 11.8$, $J/\omega_0 = 0.5$, $\omega_c/\omega_0 = 11$, and $\lambda = 0.7$.

$g = 0$. In this case it can be seen from Eq. (21) that $\mu_{g=0}^{(\text{coh})}$ is proportional to the truncation time τ and depend heavily on the structure of the energy levels, $\{E_\eta\}$,

$$\begin{aligned} \mu_{g=0}^{(\text{coh})} &= \frac{\sqrt{\pi}\tau\beta e(dJ)^2}{N_e Z_S \hbar^2} \sum_k e^{-\beta E_k} (1 - \cos 2k) \\ &= \frac{\sqrt{\pi}\tau\beta e(dJ)^2}{N_e \hbar^2} \left(1 - \sum_k \frac{e^{-\beta E_k}}{Z_S} \cos 2k \right). \end{aligned} \quad (22)$$

It is well known that the exciton-vibration coupling will give rise to the so-called band narrowing with increasing temperature, see Fig. 1 for the energy spectrum of an H-aggregate with $J/\omega_0 = 0.5$. In the high-temperature limit, $\mu_{g=0}^{(\text{coh})}$ tends to be inversely proportional to the temperature,

$$\mu_{g=0}^{(\text{coh})} \rightarrow \frac{\sqrt{\pi}\tau e(dJ)^2}{N_e k_B T}, \quad \text{as } T \rightarrow \infty, \quad (23)$$

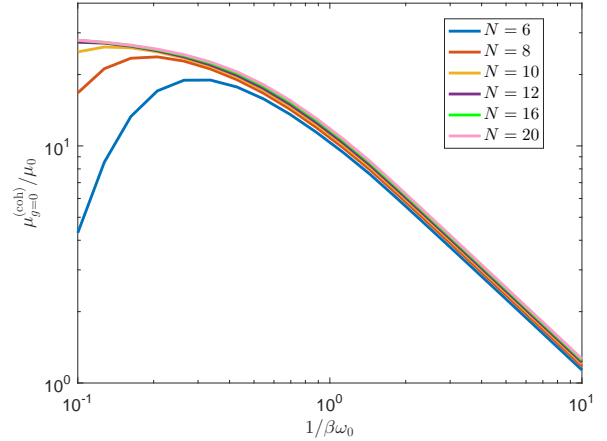


FIG. 2: Coherent mobility $\mu_{g=0}^{(\text{coh})}$ as a function of temperature for various N and $g = 0$. The truncation time is chosen as $\tau\omega_0 = 30$, and the elementary charge e and carrier number N_e are both set unit for simplicity. Other parameters: $\varepsilon_0/\omega_0 = 11.8$, $J/\omega_0 = 0.5$, $\omega_c/\omega_0 = 11$, and $\lambda = 0.7$. The unit of the mobility is $\mu_0 = ed^2/\hbar$.

since E_k becomes dispersionless. This is illustrated in Fig. 2, where $\mu_{g=0}^{(\text{coh})}$ (in unit of $\mu_0 \equiv ed^2/\hbar$) as a function of the dimensionless temperature $1/\beta\omega_0$ is shown for different temperatures. Note that $\mu_{g=0}^{(\text{coh})}$ is a non-monotonic function of T for short chains with $N \leq 10$. The suppression of the coherent mobility at low temperatures can be understood from the fact that the energy gap between different energy levels is too large to provide efficient transport channels due to the low thermal excitations of excitonic states. Note that convergent results are observed for $N > 16$.

We now turn to discuss the effects of finite exciton-cavity interaction on the coherent mobility in both the H-aggregate ($J > 0$) and J-aggregate ($J < 0$). It is known that the absorption spectrum of an H-aggregate (J-aggregate) exhibit blue (red) shift relative to the monomer excitation energy in the absence of the exciton-cavity coupling [40, 41]. Figure 3(a) shows the dispersions of a H- and J-aggregate with $N = 16$ number of sites for a strong exciton-cavity coupling $g\sqrt{N}/\omega_0 = 1$ and at a temperature with $1/\beta\omega_0 = 0.1$. The uppermost red (lowermost black) lines indicate the energy level of the upper (lower) polaron polariton [31].

In Fig. 4(a) we present the reduced coherent mobility $\mu_{g=0}^{(\text{coh})}/\mu_0$ for an H-aggregate as a function of temperature in the presence of the exciton-cavity coupling. With increasing exciton-cavity coupling, the coherent mobility first increases and then decreases after passing a crossover cavity coupling around $g\sqrt{N}/\omega_0 = 1$. This intriguing nonmonotonic behavior can be understood by investigating the evolution of the spectrum of an H-aggregate with $g\sqrt{N}/\omega_0$ [Fig. 3(b)]. It can be seen that there is a intersection between the energy levels of the lower polaron polariton and the lowest dark exciton state

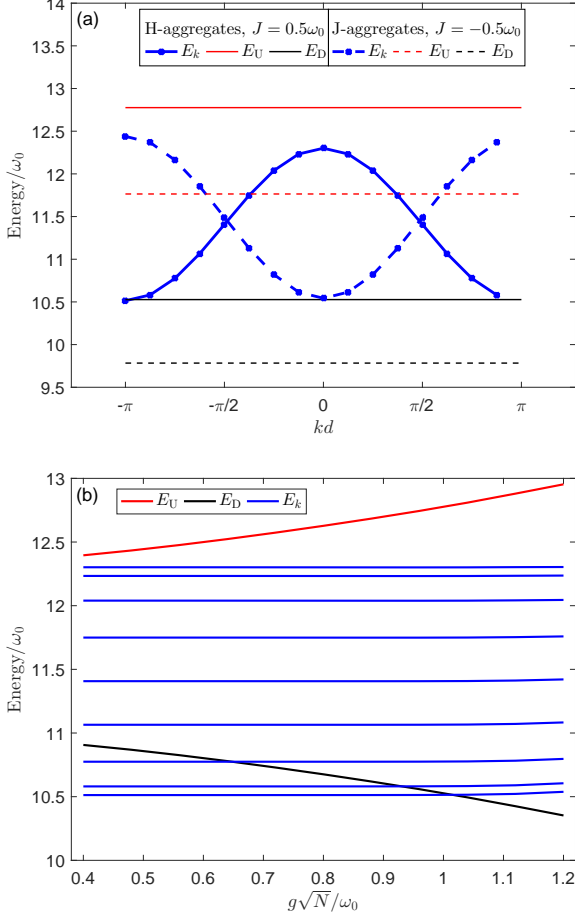


FIG. 3: (a) Dispersions of the H-aggregate ($J/\omega_0 = 0.5$, solid curve) and J-aggregate ($J/\omega_0 = -0.5$, dashed curve) for a low temperature $1/\beta\omega_0 = 0.1$ and strong cavity-exciton coupling strength $g\sqrt{N}/\omega_0 = 1$. The straight lines correspond to the upper (red) and lower (black) polaron polariton, respectively. (b) Evolution of the energy levels with $g\sqrt{N}/\omega_0$ for an H-aggregate with $J/\omega_0 = 0.5$ at a low temperature $1/\beta\omega_0 = 0.1$. Other parameters: $N = 16$, $\tau\omega_0 = 30$, $\varepsilon_0/\omega_0 = 11.8$, $\omega_c/\omega_0 = 11$, and $\lambda = 0.7$.

$|k = -\pi\rangle = a_{-\pi}^\dagger|\text{vac}\rangle$ at $g\sqrt{N}/\omega_0 \approx 1$, while the upper polaron polariton level is always well separated from the dark-exciton band. However, we see from the last term of Eq. (21) that only those terms with \mathcal{E}_η close to E_U or E_D have significant contribution to the sum over η , indicating that the lower polaron polariton state serves as a main transmission channel for an H-aggregate. As $g\sqrt{N}/\omega_0$ increases from a relatively small value, E_D will experience several intersections with the dark exciton levels having decreasing energies, which lead to an enhancement in the coherent mobility due the increasing of the thermal factor $e^{-\beta\mathcal{E}_\eta}$. After passing the last intersection with the lowest dark exciton level, E_D becomes separated from the dark exciton band, resulting in a drop of the coherent mobility with increasing $g\sqrt{N}/\omega_0$.

A similar analysis can also be applied to the case of

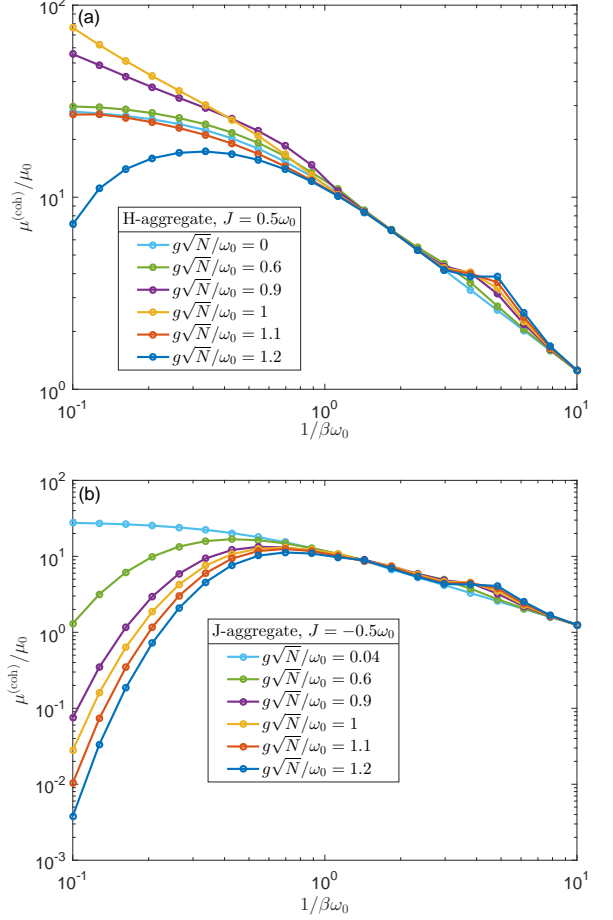


FIG. 4: Coherent mobility of (a) an H-aggregate with $J/\omega_0 = 0.5$, (b) a J-aggregate with $J/\omega_0 = -0.5$ for various values of $g\sqrt{N}/\omega_0$. Other parameters: $N = 16$, $\tau\omega_0 = 30$, $\varepsilon_0/\omega_0 = 11.8$, $\omega_c/\omega_0 = 10.5$, and $\lambda = 0.7$.

a J-aggregate. It turns out that E_D is separated from the dark exciton band and the upper polaron polariton level is the main transfer channel. This explains the monotonic decreasing of the coherent mobility for the J-aggregates shown in Fig. 3(b). At high temperatures all levels are approximately equally weighted, leading to a coherent mobility insensitive to the exciton-cavity coupling for both the H- and J-aggregate.

B. Total mobility

We now discuss the effect of exciton-cavity coupling on the total mobility of the molecular aggregates. Figure 5(a) [(b)] shows the total mobility as a function of temperature for the H-aggregate (J-aggregate). At low temperatures, the evolution of the total mobility with increasing g behaves similarly to that of the coherent mobility since the vibrational effects is minor. Similar to the case of vanishing exciton-cavity coupling [15, 16], a local

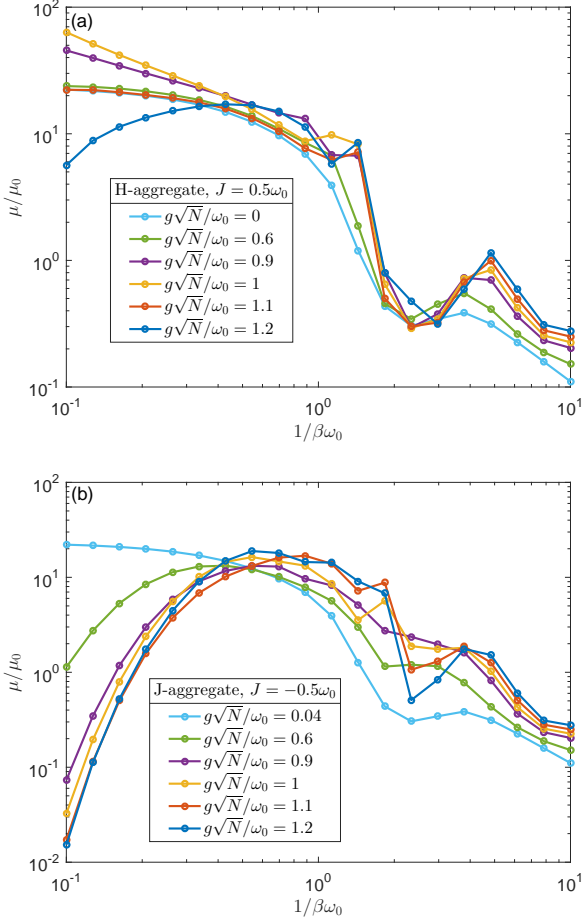


FIG. 5: Total exciton mobility of (a) an H-aggregate with $J = \omega_0 = 0.5$, (b) a J-aggregate with $J = \omega_0 = -0.5$ for various values of $g\sqrt{N}/\omega_0$. Other parameters: $N = 16$, $\tau\omega_0 = 30$, $\varepsilon_0/\omega_0 = 11.8$, $\omega_c/\omega_0 = 10.5$, and $\lambda = 0.7$.

maximum is observed in the high-temperature regime, which can be interpreted as the incoherent transport via polaron hopping. Interestingly, for both the H- and J-aggregate the total mobility exhibits a monotonic increase with increasing g in the high temperature regime. This might be due to the cavity-induced enhancement of the vibrational dressing of the cavity mode (measured by the parameter h) [31], which enters the thermal average of the vibrational operators appearing in the correlations $\langle \tilde{\mathcal{J}}_a(t) \tilde{\mathcal{J}}_c \rangle_{\tilde{H}}$, $\langle \tilde{\mathcal{J}}_c(t) \tilde{\mathcal{J}}_a \rangle_{\tilde{H}}$, and $\langle \tilde{\mathcal{J}}_c(t) \tilde{\mathcal{J}}_c \rangle_{\tilde{H}}$.

Similar to the coherent mobility, at low temperatures the total mobility also depend nonmonotonically on the exciton-cavity coupling. To illustrate this, we show in Fig. 6 the total mobility as a function of $g\sqrt{N}/\omega_0$ at room temperature ($T = 298$ K) for an H-aggregate with $J/\omega_0 = 0.5$. For each of the λ considered, there always exists an optimal exciton-cavity coupling strength $g = g_{\text{opt}}$ at which the mobility reaches a maximum. Moreover, both g_{opt} and the corresponding optimal mobility increase with increasing λ . To qualitatively un-

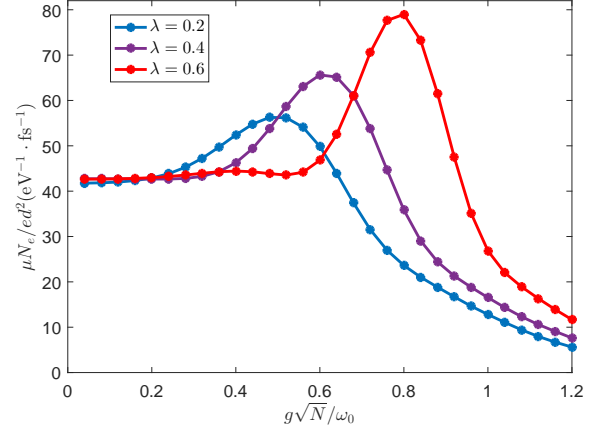


FIG. 6: The total mobility of an H-aggregate as a function of $g\sqrt{N}/\omega_0$ at temperature $T = 298$ K and for $\lambda = 0.2, 0.4$, and 0.6 . Parameters: $N = 16$, $J = 0.5\omega_0$, $\omega_c = 1.85$ eV, $\varepsilon_0 = 2$ eV, and $\omega_0 = 0.17$ eV, and $\tau = 100$ fs.

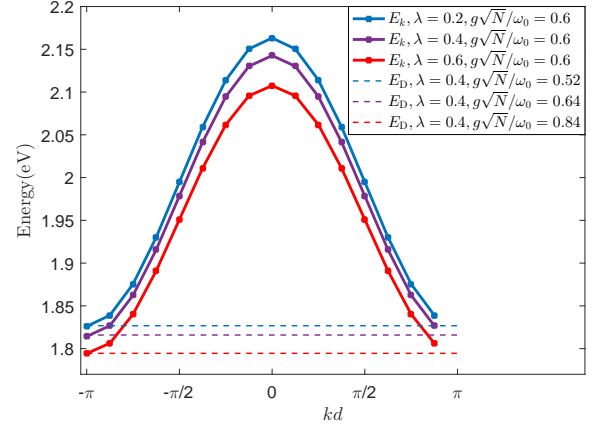


FIG. 7: The solid curves show the dark exciton dispersion for $g\sqrt{N}/\omega_0 = 0.6$ and $\lambda = 0.2, 0.4$, and 0.6 . The three dashed lines represent the lower polaron polariton level E_D for a fixed $\lambda = 0.4$ and $g\sqrt{N}/\omega_0 = 0.52, 0.64$, and 0.84 . Other parameters are the same as those in Fig. 6.

derstand these phenomena, let us look at the evolution of the dispersion when λ and g are varied. From numerical check we find that the energy levels of the dark excitons are insensitive to the change of g for fixed λ [see Fig. 3(b)], while the energy of the lower polaron polariton E_D is insensitive to the change of λ for fixed g . We thus present in Fig. (7) the dark exciton dispersions at a fixed exciton-cavity coupling $g\sqrt{N}/\omega_0 = 0.6$ and for $\lambda = 0.2, 0.4$, and 0.6 (solid curves). We also plot the lower polaron polariton level E_D for a fixed $\lambda = 0.4$ and $g\sqrt{N}/\omega_0 = 0.52, 0.64$, and 0.84 (dashed lines), in order to make these energies consistent with the corresponding lowest dark exciton energies (with $k = -\pi$). It can be seen that the three values of $g\sqrt{N}/\omega_0$ roughly

give the corresponding optimal exciton-cavity coupling g_{opt} shown in Fig. (6). Actually, the system lies in the low temperature regime and the observed mobility can qualitatively be captured by coherent mobility given by Eq. (21). To understand the enhancement of the optimal mobility with increasing λ , we first note from Eq. (21) that the cavity contribution to the coherent mobility is proportional to g_{opt}^2 , which increases as λ increases. We also note that the dark exciton band moves down as λ increases, which results in a larger thermal occupation of the lowest dark exciton state.

V. CONCLUSIONS

In this work, we present a microscopic theory for exciton transport in organic molecular crystals interacting with a single-mode cavity. Starting with the Holstein-Tavis-Cummings model, we employ a generalized Merrifield transformation developed in Ref. [31] to treat the system and obtained an expression for the exciton mobility based on the Kubo formula. As a generalization of the Cheng-Silbey [15] method that deals with charge-carrier transport in molecular crystals without a cavity,

our generalized variational canonical transformation not only takes into account the dressing of an exciton by neighboring vibrations, but also the vibrational dressing of the cavity mode. The method is believed to be capable of covering a wide range of parameters and temperatures.

Using the zeroth order of the exciton-vibration coupling, we derive a closed-form expression for the coherent contribution to the total mobility, which determines the behavior of the total mobility at low temperatures. Using the developed formalism, we perform numerical simulations on both the one-dimensional H- and J-aggregates. It is found that the exciton-cavity coupling can influence the transport properties in a significant way. Specifically, we find that for the H-aggregate there exists an optimal exciton-cavity coupling strength at which the total mobility is maximized, while for the J-aggregate the mobility decreases monotonically with increasing exciton-cavity coupling. However, an enhancement of the mobility is observed for both types of aggregates in the high temperature limit.

Acknowledgements: This work was supported by the NSFC under Grant No. 11705007 and No. 11675014, and partially by the Beijing Institute of Technology Research Fund Program for Young Scholars.

Appendix A: Calculation of current-current correlation function Eq. (16)

Using the approximated Hamiltonian $\tilde{H} \approx \tilde{H}_0$, the term $\langle \tilde{\mathcal{J}}_a(t) \tilde{\mathcal{J}}_a \rangle_{\tilde{H}}$ can be calculated as

$$\begin{aligned} \langle \tilde{\mathcal{J}}_a(t) \tilde{\mathcal{J}}_a \rangle_{\tilde{H}} &= -(edJ)^2 \sum_{jj'} \langle a_j^\dagger(t) a_{j+1}(t) a_{j'}^\dagger, a_{j'+1} \rangle_{\tilde{H}_S} \langle e^{B_{j+1}(t)-B_j(t)} e^{B_{j'+1}-B_{j'}} \rangle_{H_V} \\ &+ (edJ)^2 \sum_{jj'} \langle a_j^\dagger(t) a_{j+1}(t) a_{j'+1}^\dagger, a_{j'} \rangle_{\tilde{H}_S} \langle e^{B_{j+1}(t)-B_j(t)} e^{B_{j'}-B_{j'+1}} \rangle_{H_V} \\ &+ (edJ)^2 \sum_{jj'} \langle a_{j+1}^\dagger(t) a_j(t) a_{j'}^\dagger, a_{j'+1} \rangle_{\tilde{H}_S} \langle e^{B_j(t)-B_{j+1}(t)} e^{B_{j'+1}-B_{j'}} \rangle_{H_V} \\ &- (edJ)^2 \sum_{jj'} \langle a_{j+1}^\dagger(t) a_j(t) a_{j'+1}^\dagger, a_{j'} \rangle_{\tilde{H}_S} \langle e^{B_j(t)-B_{j+1}(t)} e^{B_{j'}-B_{j'+1}} \rangle_{H_V}. \end{aligned} \quad (\text{A1})$$

We thus need to calculate

$$\langle a_r^\dagger(t) a_l(t) a_m^\dagger a_n \rangle_{\tilde{H}_S} = \frac{1}{N^2} \sum_{\eta\eta'\eta''\eta'''} e^{-iK_\eta r + i\varepsilon_\eta t} x_\eta e^{iK_{\eta'} l - i\varepsilon_{\eta'} t} x_{\eta'} e^{-iK_{\eta''} m} x_{\eta''} e^{iK_{\eta'''} n} x_{\eta'''} \langle f_\eta^\dagger f_{\eta'} f_{\eta''}^\dagger f_{\eta'''} \rangle_{\tilde{H}_S}, \quad (\text{A2})$$

where we used $a_j(t) = \frac{1}{\sqrt{N}} \sum_{\eta=1}^{N+1} e^{iK_\eta j - i\varepsilon_\eta t} x_\eta f_\eta$ and $c(t) = \sum_{\eta=1}^{N+1} e^{-i\varepsilon_\eta t} y_\eta f_\eta$. Recall that $f_\eta f_{\eta'}^\dagger = |\text{vac}\rangle \langle \eta | \eta' \rangle \langle \text{vac}| = \delta_{\eta\eta'} |\text{vac}\rangle \langle \text{vac}|$, and $f_\eta^\dagger f_{\eta'} = |\eta\rangle \langle \text{vac}| \langle \text{vac}| \langle \eta'| = |\eta\rangle \langle \eta'|$, so $f_\eta^\dagger f_{\eta'} f_{\eta''}^\dagger f_{\eta'''} = |\eta\rangle \langle \eta' | \eta'' \rangle \langle \eta'''| = \delta_{\eta'\eta''} |\eta\rangle \langle \eta'''|$, yielding

$$\langle f_\eta^\dagger f_{\eta'} f_{\eta''}^\dagger f_{\eta'''} \rangle_{\tilde{H}_S} = \frac{1}{Z_S} \delta_{\eta'\eta''} \text{Tr}_S(e^{-\beta \tilde{H}_S} |\eta\rangle \langle \eta'''|) = \frac{1}{Z_S} \delta_{\eta'\eta''} \sum_\chi e^{-\beta E_\chi} \langle \chi | \eta \rangle \langle \eta''' | \chi \rangle = \frac{e^{-\beta E_\eta}}{Z_S} \delta_{\eta'\eta''} \delta_{\eta\eta''}. \quad (\text{A3})$$

Inserting Eq. (A3) into Eq. (A2), we have

$$\langle a_r^\dagger(t) a_l(t) a_m^\dagger a_n \rangle_{\tilde{H}_S} = \frac{1}{Z_S N^2} \sum_\eta e^{-\beta E_\eta} x_\eta^2 e^{-iK_\eta(r-n) + i\varepsilon_\eta t} \sum_{\eta'} x_{\eta'}^2 e^{iK_{\eta'}(l-m) - i\varepsilon_{\eta'} t}. \quad (\text{A4})$$

Another quantity we need to calculate is thermal average of the vibrational operators

$$\langle e^{B_l(t)-B_r(t)} e^{B_n-B_m} \rangle_{H_V} = e^{-\frac{1}{2}\Phi_{\omega_0}(0)} \sum_s [(f_{s-l}-f_{s-r})^2 + (f_{s-n}-f_{s-m})^2] e^{-\Phi_{\omega_0}(t)} \sum_s [(f_{s-l}-f_{s-r})(f_{s-n}-f_{s-m})], \quad (\text{A5})$$

where $\Phi_{\omega_0}(t) = n_{\omega_0} e^{i\omega_0 t} + (1 + n_{\omega_0}) e^{-i\omega_0 t}$ with $n_{\omega_0} = 1/(e^{\beta\omega_0} - 1)$ the Bose-Einstein distribution function.

For thermal averages involving B_j , we only need to replace the f by h in the above equation, e.g.,

$$\langle e^{B_c(t) - B_r(t)} e^{B_n - B_m} \rangle_{H_v} = e^{-\frac{1}{2}\Phi_{\omega_0}(0) \sum_s [(h - f_{s-r})^2 + (f_{s-n} - f_{s-m})^2]} e^{-\Phi_{\omega_0}(t) \sum_s [(h - f_{s-r})(f_{s-n} - f_{s-m})]}. \quad (\text{A6})$$

The cross term can be calculated as

$$\begin{aligned} \langle \tilde{\mathcal{J}}_a(t) \tilde{\mathcal{J}}_c \rangle_{\tilde{H}} &= e^2 dJg \sum_{jj'} R_{j'} \langle a_j^\dagger(t) a_{j+1}(t) a_{j'}^\dagger c \rangle_{\tilde{H}_S} \langle e^{B_{j+1}(t) - B_j(t)} e^{B_c - B_{j'}} \rangle_{\tilde{H}_v} \\ &\quad - e^2 dJg \sum_{jj'} R_{j'} \langle a_j^\dagger(t) a_{j+1}(t) c^\dagger a_{j'} \rangle_{\tilde{H}_S} \langle e^{B_{j+1}(t) - B_j(t)} e^{B_{j'} - B_c} \rangle_{\tilde{H}_v} \\ &\quad - e^2 dJg \sum_{jj'} R_{j'} \langle a_{j+1}^\dagger(t) a_j(t) a_{j'}^\dagger c \rangle_{\tilde{H}_S} \langle e^{B_j(t) - B_{j+1}(t)} e^{B_c - B_{j'}} \rangle_{\tilde{H}_v} \\ &\quad + e^2 dJg \sum_{jj'} R_{j'} \langle a_{j+1}^\dagger(t) a_j(t) c^\dagger a_{j'} \rangle_{\tilde{H}_S} \langle e^{B_j(t) - B_{j+1}(t)} e^{B_{j'} - B_c} \rangle_{\tilde{H}_v}. \end{aligned} \quad (\text{A7})$$

The two types of the thermal averages of the exciton-photon operators are

$$\begin{aligned} \langle a_r^\dagger(t) a_l(t) a_m^\dagger c \rangle_{\tilde{H}_S} &= \frac{1}{Z_S N \sqrt{N}} \sum_{\eta} e^{-\beta \mathcal{E}_{\eta}} x_{\eta} y_{\eta} e^{-iK_{\eta} r + i\mathcal{E}_{\eta} t} \sum_{\eta'} x_{\eta'}^2 e^{iK_{\eta'}(l-m) - i\mathcal{E}_{\eta'} t}, \\ \langle a_r^\dagger(t) a_l(t) c^\dagger a_n \rangle_{\tilde{H}_S} &= \frac{1}{Z_S N \sqrt{N}} \sum_{\eta} e^{-\beta \mathcal{E}_{\eta}} x_{\eta}^2 e^{-iK_{\eta}(r-n) + i\mathcal{E}_{\eta} t} \sum_{\eta'} x_{\eta'} y_{\eta'} e^{iK_{\eta'} l - i\mathcal{E}_{\eta'} t}. \end{aligned} \quad (\text{A8})$$

Similarly,

$$\begin{aligned} \langle \tilde{\mathcal{J}}_c(t) \tilde{\mathcal{J}}_a \rangle_{\tilde{H}} &= e^2 dJg \sum_{jj'} R_j \langle a_j^\dagger(t) c(t) a_{j'}^\dagger a_{j'+1} \rangle_{\tilde{H}_S} \langle e^{B_c(t) - B_j(t)} e^{B_{j'+1} - B_{j'}} \rangle_{\tilde{H}_v} \\ &\quad - e^2 dJg \sum_{jj'} R_j \langle a_j^\dagger(t) c(t) a_{j'+1}^\dagger a_{j'} \rangle_{\tilde{H}_S} \langle e^{B_c(t) - B_j(t)} e^{B_{j'} - B_{j'+1}} \rangle_{\tilde{H}_v} \\ &\quad - e^2 dJg \sum_{jj'} R_j \langle c^\dagger(t) a_j(t) a_{j'}^\dagger a_{j'+1} \rangle_{\tilde{H}_S} \langle e^{B_j(t) - B_c(t)} e^{B_{j'+1} - B_{j'}} \rangle_{\tilde{H}_v} \\ &\quad + e^2 dJg \sum_{jj'} R_j \langle c^\dagger(t) a_j(t) a_{j'+1}^\dagger a_{j'} \rangle_{\tilde{H}_S} \langle e^{B_j(t) - B_c(t)} e^{B_{j'} - B_{j'+1}} \rangle_{\tilde{H}_v}, \end{aligned} \quad (\text{A9})$$

with

$$\begin{aligned} \langle c^\dagger(t) a_l(t) a_m^\dagger a_n \rangle_{\tilde{H}_S} &= \frac{1}{Z_S N \sqrt{N}} \sum_{\eta} e^{-\beta \mathcal{E}_{\eta}} x_{\eta} y_{\eta} e^{iK_{\eta} n + i\mathcal{E}_{\eta} t} \sum_{\eta'} x_{\eta'}^2 e^{iK_{\eta'}(l-m) - i\mathcal{E}_{\eta'} t}, \\ \langle a_r^\dagger(t) c(t) a_m^\dagger a_n \rangle_{\tilde{H}_S} &= \frac{1}{Z_S N \sqrt{N}} \sum_{\eta} e^{-\beta \mathcal{E}_{\eta}} x_{\eta}^2 e^{-iK_{\eta}(r-n) + i\mathcal{E}_{\eta} t} \sum_{\eta'} x_{\eta'} y_{\eta'} e^{-iK_{\eta'} m - i\mathcal{E}_{\eta'} t}. \end{aligned} \quad (\text{A10})$$

The last term can be calculated as

$$\begin{aligned} \langle \tilde{\mathcal{J}}_c(t) \tilde{\mathcal{J}}_c \rangle_{\tilde{H}} &= -(eg)^2 \sum_{j=1}^N \sum_{j'=1}^N \langle R_j R_{j'} [a_j^\dagger(t) c(t) e^{B_c(t) - B_j(t)} - e^{B_j(t) - B_c(t)} c^\dagger(t) a_j(t)] [a_j^\dagger c e^{B_c - B_{j'}} - e^{B_{j'} - B_c} c^\dagger a_{j'}] \rangle_{\tilde{H}} \\ &= -(eg)^2 \sum_{jj'} R_j R_{j'} \langle a_j^\dagger(t) c(t) a_{j'}^\dagger c \rangle_{\tilde{H}_S} \langle e^{B_c(t) - B_j(t)} e^{B_c - B_{j'}} \rangle_{H_v} \\ &\quad + (eg)^2 \sum_{jj'} R_j R_{j'} \langle a_j^\dagger(t) c(t) c^\dagger a_{j'} \rangle_{\tilde{H}_S} \langle e^{B_c(t) - B_j(t)} e^{B_{j'} - B_c} \rangle_{H_v} \\ &\quad + (eg)^2 \sum_{jj'} R_j R_{j'} \langle c^\dagger(t) a_j(t) a_{j'}^\dagger c \rangle_{\tilde{H}_S} \langle e^{B_j(t) - B_c(t)} e^{B_c - B_{j'}} \rangle_{H_v} \\ &\quad - (eg)^2 \sum_{jj'} R_j R_{j'} \langle c^\dagger(t) a_j(t) c^\dagger a_{j'} \rangle_{\tilde{H}_S} \langle e^{B_j(t) - B_c(t)} e^{B_{j'} - B_c} \rangle_{H_v}, \end{aligned} \quad (\text{A11})$$

where

$$\begin{aligned}
\langle a_r^\dagger(t)c(t)a_m^\dagger c \rangle_{\tilde{H}_S} &= \frac{1}{Z_S N} \sum_{\eta} e^{-\beta \varepsilon_{\eta}} x_{\eta} y_{\eta} e^{-iK_{\eta} r + i\varepsilon_{\eta} t} \sum_{\eta'} x_{\eta'} y_{\eta'} e^{-iK_{\eta'} m - i\varepsilon_{\eta'} t}, \\
\langle a_r^\dagger(t)c(t)c^\dagger a_n \rangle_{\tilde{H}_S} &= \frac{1}{Z_S N} \sum_{\eta} e^{-\beta \varepsilon_{\eta}} x_{\eta}^2 e^{-iK_{\eta}(r-n) + i\varepsilon_{\eta} t} \sum_{\eta'} y_{\eta'}^2 e^{-i\varepsilon_{\eta'} t}, \\
\langle c^\dagger(t)a_l(t)a_m^\dagger c \rangle_{\tilde{H}_S} &= \frac{1}{Z_S N} \sum_{\eta} e^{-\beta \varepsilon_{\eta}} y_{\eta}^2 e^{i\varepsilon_{\eta} t} \sum_{\eta'} x_{\eta'}^2 e^{iK_{\eta'}(l-m) - i\varepsilon_{\eta'} t}, \\
\langle c^\dagger(t)a_l(t)c^\dagger a_n \rangle_{\tilde{H}_S} &= \frac{1}{Z_S N} \sum_{\eta} e^{-\beta \varepsilon_{\eta}} x_{\eta} y_{\eta} e^{iK_{\eta} n + i\varepsilon_{\eta} t} \sum_{\eta'} x_{\eta'} y_{\eta'} e^{iK_{\eta'} l - i\varepsilon_{\eta'} t}.
\end{aligned} \tag{A12}$$

Appendix B: Calculation of the coherent mobility $\mu^{(\text{coh})}$

We derive the explicit expression for the coherent contribution to the mobility, which is obtained by setting all thermal averages of the vibrational operator in Appendix A to be 1. The four terms are:

1)

$$\begin{aligned}
\langle \tilde{\mathcal{J}}_a(t) \tilde{\mathcal{J}}_a \rangle_{\tilde{H}}^{(\text{coh})} &= -(edJ)^2 \sum_{jj'} [\langle a_j^\dagger(t) a_{j+1}(t) a_j^\dagger a_{j+1} \rangle_{\tilde{H}_S} - \langle a_j^\dagger(t) a_{j+1}(t) a_{j'+1}^\dagger a_{j'} \rangle_{\tilde{H}_S} \\
&\quad - \langle a_{j+1}^\dagger(t) a_j(t) a_j^\dagger a_{j+1} \rangle_{\tilde{H}_S} + \langle a_{j+1}^\dagger(t) a_j(t) a_{j'+1}^\dagger a_{j'} \rangle_{\tilde{H}_S}] \\
&= -(edJ)^2 \frac{1}{Z_S} \sum_{\eta=1}^{N-1} e^{-\beta E_{\eta}} 2(\cos 2K_{\eta} - 1)
\end{aligned} \tag{B1}$$

2)

$$\begin{aligned}
\langle \tilde{\mathcal{J}}_a(t) \tilde{\mathcal{J}}_c \rangle_{\tilde{H}}^{(\text{coh})} &= e^2 dJg \sum_{jj'} R_{j'} [\langle a_j^\dagger(t) a_{j+1}(t) a_j^\dagger c \rangle_{\tilde{H}_S} - \langle a_j^\dagger(t) a_{j+1}(t) c^\dagger a_{j'} \rangle_{\tilde{H}_S} \\
&\quad - \langle a_{j+1}^\dagger(t) a_j(t) a_j^\dagger c \rangle_{\tilde{H}_S} + \langle a_{j+1}^\dagger(t) a_j(t) c^\dagger a_{j'} \rangle_{\tilde{H}_S}] \\
&= e^2 dJg \sum_{j'} R_{j'} \frac{1}{Z_S \sqrt{N}} \sum_{\eta, \eta' = N, N+1} e^{-\beta \varepsilon_{\eta}} e^{i(\varepsilon_{\eta} - \varepsilon_{\eta'}) t} (x_{\eta} y_{\eta} x_{\eta'}^2 - x_{\eta} y_{\eta} x_{\eta'}^2 - x_{\eta}^2 x_{\eta'} y_{\eta'} + x_{\eta}^2 x_{\eta'} y_{\eta'}) \\
&= 0.
\end{aligned} \tag{B2}$$

One can similarly show that $\langle \tilde{\mathcal{J}}_a(t) \tilde{\mathcal{J}}_c \rangle_{\tilde{H}}^{(\text{coh})} = 0$.

3)

$$\begin{aligned}
\langle \tilde{\mathcal{J}}_c(t) \tilde{\mathcal{J}}_c \rangle_{\tilde{H}} &= -(eg)^2 \sum_{jj'} R_j R_{j'} [\langle a_j^\dagger(t) c(t) a_j^\dagger c \rangle_{\tilde{H}_S} - \langle a_j^\dagger(t) c(t) c^\dagger a_{j'} \rangle_{\tilde{H}_S} - \langle c^\dagger(t) a_j(t) a_j^\dagger c \rangle_{\tilde{H}_S} + \langle c^\dagger(t) a_j(t) c^\dagger a_{j'} \rangle_{\tilde{H}_S}] \\
&= -(eg)^2 \sum_{jj'} R_j R_{j'} \frac{1}{Z_S N} \sum_{\eta \eta'} e^{-\beta \varepsilon_{\eta}} e^{i(\varepsilon_{\eta} - \varepsilon_{\eta'}) t} \\
&\quad [x_{\eta} y_{\eta} e^{-iK_{\eta} j} x_{\eta'} y_{\eta'} e^{-iK_{\eta'} j'} - x_{\eta}^2 e^{-iK_{\eta}(j-j')} y_{\eta'}^2 - y_{\eta}^2 x_{\eta'}^2 e^{-iK_{\eta'}(j-j')} + x_{\eta} y_{\eta} e^{iK_{\eta} j'} x_{\eta'} y_{\eta'} e^{iK_{\eta'} j}] \\
&= (eg)^2 \frac{1}{Z_S N} [e^{-\beta E_U} e^{i(E_U - E_D) t} + e^{-\beta E_D} e^{i(E_D - E_U) t}] \sum_{jj'} R_j R_{j'} \\
&\quad + (eg)^2 \frac{S^2}{Z_S N} \sum_{\eta=1}^{N-1} [e^{-\beta \varepsilon_{\eta}} e^{i(\varepsilon_{\eta} - E_U) t} + e^{-\beta E_U} e^{-i(\varepsilon_{\eta} - E_U) t}] \sum_{jj'} R_j R_{j'} e^{-iK_{\eta}(j-j')} \\
&\quad + (eg)^2 \frac{C^2}{Z_S N} \sum_{\eta=1}^{N-1} [e^{-\beta \varepsilon_{\eta}} e^{i(\varepsilon_{\eta} - E_D) t} + e^{-\beta E_D} e^{-i(\varepsilon_{\eta} - E_D) t}] \sum_{jj'} R_j R_{j'} e^{-iK_{\eta}(j-j')}.
\end{aligned} \tag{B3}$$

By using $R_j = jd$, we have

$$\begin{aligned}\sum_{j=1}^N R_j &= d \sum_{j=1}^N j = d \frac{N(N+1)}{2}, \\ \sum_{j=1}^N R_j e^{-iK_\eta j} &= d \sum_{j=1}^N j e^{-iK_\eta(jd)} = d \frac{e^{-iK_\eta d N} [N - (N+1)e^{idK_\eta} + e^{i(1+N)K_\eta d}]}{(e^{idK_\eta} - 1)^2} = dN \frac{1}{1 - e^{idK_\eta}},\end{aligned}\quad (\text{B4})$$

so that

$$\begin{aligned}\sum_{jj'} R_j R_{j'} &= d^2 \frac{N^2(N+1)^2}{4}, \\ \sum_{jj'} R_j R_{j'} e^{-iK_\eta(j-j')} &= d^2 N^2 \frac{1}{(1 - e^{idK_\eta})(1 - e^{-idK_\eta})} = d^2 N^2 \frac{1}{2(1 - \cos K_\eta d)}\end{aligned}\quad (\text{B5})$$

giving

$$\begin{aligned}\langle \tilde{\mathcal{J}}_c(t) \tilde{\mathcal{J}}_c \rangle_{\tilde{H}} &= (edg)^2 \frac{N(N+1)^2}{4Z_S} [e^{-\beta E_U} e^{i(E_U - E_D)t} + e^{-\beta E_D} e^{i(E_D - E_U)t}] \\ &+ (edg)^2 \frac{NS^2}{2Z_S} \sum_{\eta=1}^{N-1} [e^{-\beta \mathcal{E}_\eta} e^{i(\mathcal{E}_\eta - E_U)t} + e^{-\beta E_U} e^{-i(\mathcal{E}_\eta - E_U)t}] \frac{1}{1 - \cos K_\eta d} \\ &+ (edg)^2 \frac{NC^2}{2Z_S} \sum_{\eta=1}^{N-1} [e^{-\beta \mathcal{E}_\eta} e^{i(\mathcal{E}_\eta - E_D)t} + e^{-\beta E_D} e^{-i(\mathcal{E}_\eta - E_D)t}] \frac{1}{1 - \cos K_\eta d}.\end{aligned}\quad (\text{B6})$$

In all, we have

$$\begin{aligned}\mu^{(\text{coh})} &= \frac{\beta}{2eN_e} \int_{-\infty}^{\infty} dt [\langle \tilde{\mathcal{J}}_a(t) \tilde{\mathcal{J}}_a \rangle_{\tilde{H}}^{\text{coh}} + \langle \tilde{\mathcal{J}}_c(t) \tilde{\mathcal{J}}_c \rangle_{\tilde{H}}^{\text{coh}}] \\ &= \frac{\beta e (dJ)^2}{N_e Z_S} \int_{-\infty}^{\infty} dt \sum_{\eta=1}^{N-1} e^{-\beta E_\eta} (1 - \cos 2K_\eta) \\ &+ \frac{\beta e (dg)^2 N(N+1)^2}{8N_e Z_S} \int_{-\infty}^{\infty} dt [e^{-\beta E_U} e^{i(E_U - E_D)t} + e^{-\beta E_D} e^{i(E_D - E_U)t}] \\ &+ \frac{\beta e (dg)^2 NS^2}{4N_e Z_S} \int_{-\infty}^{\infty} dt \sum_{\eta=1}^{N-1} [e^{-\beta \mathcal{E}_\eta} e^{i(\mathcal{E}_\eta - E_U)t} + e^{-\beta E_U} e^{-i(\mathcal{E}_\eta - E_U)t}] \frac{1}{1 - \cos K_\eta d} \\ &+ \frac{\beta e (dg)^2 NC^2}{4N_e Z_S} \int_{-\infty}^{\infty} dt \sum_{\eta=1}^{N-1} [e^{-\beta \mathcal{E}_\eta} e^{i(\mathcal{E}_\eta - E_D)t} + e^{-\beta E_D} e^{-i(\mathcal{E}_\eta - E_D)t}] \frac{1}{1 - \cos K_\eta d}.\end{aligned}\quad (\text{B7})$$

By introducing a limiting scattering time from static disorder in terms of

$$\int dt \rightarrow \int dt e^{-(t/\tau)^2}, \quad (\text{B8})$$

where τ measures the coherence time, we arrive at

$$\begin{aligned}\mu^{(\text{coh})} &= \frac{\beta}{2eN_e} \int_{-\infty}^{\infty} dt [\langle \tilde{\mathcal{J}}_a(t) \tilde{\mathcal{J}}_a \rangle_{\tilde{H}}^{\text{coh}} + \langle \tilde{\mathcal{J}}_c(t) \tilde{\mathcal{J}}_c \rangle_{\tilde{H}}^{\text{coh}}] \\ &= \frac{\sqrt{\pi} \tau \beta e (dJ)^2}{N_e Z_S} \sum_{\eta=1}^{N-1} e^{-\beta E_\eta} (1 - \cos 2K_\eta) \\ &+ \frac{\sqrt{\pi} \tau \beta e (dg)^2 N(N+1)^2}{8N_e Z_S} (e^{-\beta E_U} + e^{-\beta E_D}) e^{-\frac{1}{4}\tau^2 (E_U - E_D)^2}\end{aligned}$$

$$\begin{aligned}
& + \frac{\sqrt{\pi}\tau\beta e(dg)^2 NS^2}{4N_e Z_S} \sum_{\eta=1}^{N-1} (e^{-\beta\epsilon_\eta} + e^{-\beta E_U}) e^{-\frac{1}{4}\tau^2(\epsilon_\eta - E_U)^2} \frac{1}{1 - \cos K_\eta d} \\
& + \frac{\sqrt{\pi}\tau\beta e(dg)^2 NC^2}{4N_e Z_S} \sum_{\eta=1}^{N-1} (e^{-\beta\epsilon_\eta} + e^{-\beta E_D}) e^{-\frac{1}{4}\tau^2(\epsilon_\eta - E_D)^2} \frac{1}{1 - \cos K_\eta d}.
\end{aligned} \tag{B9}$$

-
- [1] V. Coropceanu, J. Cornil, D. A. da Silva Filho, Y. Olivier, R. Silbey, and J.-L. Brédas, *Chem. Rev.* (Washington, D.C.) **107**, 926 (2007).
- [2] S. M. Menke, W. A. Luhman, and R. J. Holmes, *Nat. Mater.* **12**, 152 (2013).
- [3] Y.-C. Cheng and G. R. Fleming, *Annu. Rev. Phys. Chem.* **60**, 241 (2009).
- [4] G. D. Scholes, G. R. Fleming, A. Olaya-Castro, and R. van Grondelle, *Nat. Chem.* **3**, 763 (2011).
- [5] M. Grover and R. Silbey, *J. Chem. Phys.* **54**, 4843 (1971).
- [6] R. Silbey, *Ann. Rev. Phys. Chem.* **27**, 203 (1976).
- [7] D. R. Yarkony and R. Silbey, *J. Chem. Phys.* **65**, 1042 (1976).
- [8] D. R. Yarkony and R. Silbey, *J. Chem. Phys.* **67**, 5818 (1977).
- [9] R. W. Munn and R. Silbey, *J. Chem. Phys.* **68**, 2439 (1977).
- [10] R. Silbey and R. W. Munn, *J. Chem. Phys.* **72**, 2763 (1980).
- [11] T. Holstein, *Ann. Phys. (N.Y.)* **8**, 325 (1959).
- [12] A. Troisi, *Chem. Soc. Rev.* **40**, 2347 (2011).
- [13] R. W. Munn and R. Silbey, *J. Chem. Phys.* **83**, 1843 (1985).
- [14] R. W. Munn and R. Silbey, *J. Chem. Phys.* **83**, 1843 (1985).
- [15] Y. C. Cheng and R. J. Silbey, *J. Chem. Phys.* **128**, 114713 (2008).
- [16] F. Ortmann, F. Bechstedt, and K. Hannewald, *Phys. Rev. B* **79**, 235206 (2009).
- [17] N. Prodanović and N. Vukmirović, *Phys. Rev. B* **99**, 104304 (2019).
- [18] E. Orgiu, J. George, J. Hutchison, E. Devaux, J. F. Dayen, B. Doudin, F. Stellacci, C. Genet, P. Samor, and T. W. Ebbesen, *Nat. Mater.* **14**, 1123 (2015).
- [19] J. Feist and F. J. Garcia-Vidal, *Phys. Rev. Lett.* **114**, 196402 (2015).
- [20] J. Schachenmayer, C. Genes, E. Tignone, and G. Pupillo, *Phys. Rev. Lett.* **114**, 196403 (2015).
- [21] J. Yuen-Zhou, S. K. Saikin, T. Zhu, M. Onbalsi, C. Ross, V. Bulovic, and M. Baldo, *Nat. Commun.* **7**, 11783 (2016).
- [22] D. Hagenmüller, J. Schachenmayer, S. Schtz, C. Genes, and G. Pupillo, *Phys. Rev. Lett.* **119**, 223601 (2017).
- [23] X. Zhong, T. Chervy, L. Zhang, A. Thomas, J. George, C. Genet, J. A. Hutchison, and T. W. Ebbesen, *Angew. Chem., Int. Ed.* **56**, 9034 (2017).
- [24] M. Du, L. A. Martínez-Martínez, R. F. Ribeiro, Z. Hu, V. M. Menon, and J. Yuen-Zhou, *Chem. Sci.* **9**, 6659 (2018).
- [25] R. Sáez-Blázquez, J. Feist, A. I. Fernández-Domínguez, and F. J. García-Vidal, *Phys. Rev. B* **97**, 241407 (2018).
- [26] J. Liu, Q. Zhao, and N. Wu, *J. Chem. Phys.* **150**, 105102 (2019).
- [27] J. Wei, F. Zhao, J. Liu, Q. Zhao, N. Wu, and D. Xu, *Phys. Rev. E* **100**, 012125 (2019).
- [28] M. A. Zeb, P. G. Kirton, and J. Keeling, arXiv: 2004.09790.
- [29] J. A. Ćwik, S. Reja, P. B. Littlewood, and J. Keeling, *Europhys. Lett.* **105**, 47009 (2014).
- [30] F. C. Spano, *J. Chem. Phys.* **142**, 184707 (2015).
- [31] N. Wu, J. Feist, and F. J. Garcia-Vidal, *Phys. Rev. B* **94**, 195409 (2016).
- [32] M. A. Zeb, P. G. Kirton, and J. Keeling, *ACS Photonics* **5**, 249 (2017).
- [33] L. A. Martínez, E. Eizner, S. Kéna-Cohen, and J. Yuen-Zhou, *J. Chem. Phys.* **151**, 054106 (2019).
- [34] N. J. Hestand and F. C. Spano, *Chem. Rev.* **118**, 7069 (2018).
- [35] K. Mukai, S. Abe, and H. Sumi, *J. Phys. Chem. B* **103**, 6096 (1999).
- [36] A. Damjanović, I. Kosztin, U. Kleinekathöfer, and K. Schulten, *Phys. Rev. E* **65**, 031919 (2002).
- [37] We assume the size of the aggregate is much smaller than the cavity wavelength, see Ref. [27] for the effect of inhomogeneous exciton-cavity coupling on the exciton transport in molecular aggregates.
- [38] R. P. Feynman, *Statistical Mechanics: A Set Of Lectures*, Advanced Book Classics (Westview, Boulder, CO, 1998).
- [39] G. D. Mahan, *Many-Particle Physics* (Kluwer Academic Publishers, New York, 2000).
- [40] F. C. Spano, *Acc. Chem. Res.* **43**, 429 (2010).
- [41] F. C. Spano and C. Silva, *Annu. Rev. Phys. Chem.* **65**, 477 (2014).